

Chemistry of vibronic coupling. Part 1: How to maximize vibronic coupling constants in a diabatic harmonic potential model?

Wojciech Grochala¹, Robert Konecny, Roald Hoffmann^{*}

Department of Chemistry and Chemical Biology, Cornell University, Ithaca, NY 14850, USA

Received 21 April 2000

Abstract

Using a simple diabatic model of two equivalent energy minima with crossing harmonic potential energy surfaces, we analyze the vibronic coupling constant λ_{eg}^i ($e, g \equiv$ electronic states coupled, $i \equiv$ coupling vibration). λ_{eg}^i (expressed in energy units) is a product of h_{eg}^i (expressed in force units) and $\langle u_g | Q_i | v_e \rangle$ (expressed in distance units) where h_{eg}^i is the dynamic off-diagonal vibronic coupling constant, u_g and v_e are vibrational wave functions for normal mode i , in the g and e state respectively, and Q_i is normal coordinate of i th mode. We study the way λ_{eg}^i depends on three parameters: the force constant (k), the reduced oscillator mass (m) and the displacement between two minima along the normal coordinate of the coupling mode Q_i (ΔQ). For each k there is only one ΔQ which maximizes λ_{eg}^i . The maximum in λ_{eg}^i originates from the opposing behavior of h_{eg}^i and $\langle g | \delta H / \delta Q_i | e \rangle$ factors in $(k, \Delta Q)$ space. A strategy for obtaining large λ_{eg}^i s should adjust properly small ΔQ s in systems with strong multiple bonds (large k s). This condition appears to be hard to fulfill in experiment. It also emerges that λ_{eg}^i correlates linearly with $\sqrt{(k/m)}$. Hence, to maximize λ_{eg}^i one should build a system of light elements. The results presented here may be useful in the experimental search for high-temperature superconductivity, delimiting the space of element combinations which might be investigated. © 2001 Published by Elsevier Science B.V.

1. Introduction

The vibronic coupling constant (VCC) is an important molecular parameter which describes in a quantitative way the phenomenon of vibrational coupling of electronic states.² Interest in VCCs increased substantially when the BCS theory of superconductivity was born [5], because of the fun-

damental role of electron–phonon coupling in that theory. Although it is clear that the community lost some faith in the explanative role of classical BCS theory after discovery of high-temperature superconductivity (HTSC) [6] in early '80s, both theoretical and experimental investigations of VCCs are common in literature [7,8]. Despite many (contradictory) claims by proponents of this or that theory, the HTSC phenomenon remains till today quite mysterious. Also few of the many competing theoretical approaches can be easily translated into chemical language.

Our investigations also have their source in the phenomenon of superconductivity. Although BCS

^{*} Corresponding author. Fax: +1-607-255-5707.

E-mail address: rh34@cornell.edu (R. Hoffmann).

¹ Also corresponding author.

² On the theory of vibronic coupling see Refs. [1–4].

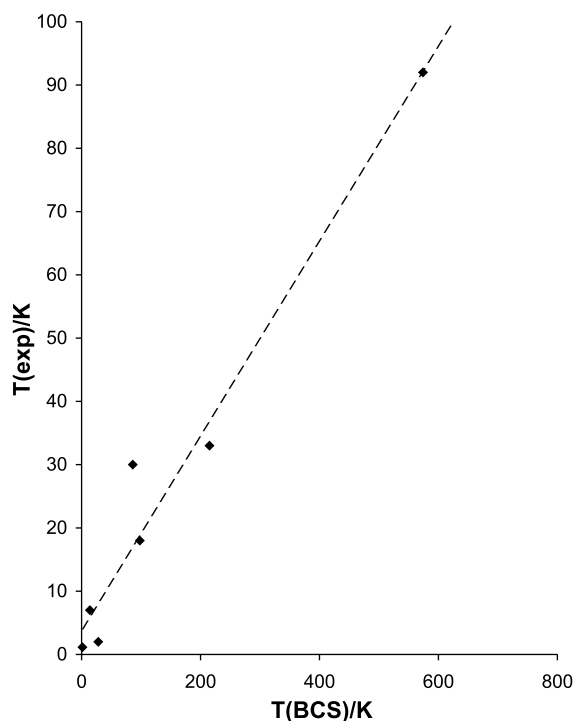


Fig. 1. Correlation of T_c predicted by BCS theory with the experimental value of T_c . Numerical data for the points shown (Al, Pb, K_3C_{60} , $Li_{0.9}Mo_6O_{17}$, $Ba_{0.6}K_{0.4}BiO_3$, $LaSr_{0.15}CuO_4$ and YBCO superconductors) are taken from Ref. [8].

theory does not allow a quantitative prediction of the onset and parameters of HTSC, there still exists a qualitative correlation between experimental values of the critical temperature (T_c) and those calculated within the BCS theory [9] up to 100 K (see Fig. 1). BCS theory deals with the full polaron coupling problem, including terms that are both diagonal and off-diagonal in the local electronic populations. Since BCS predicts higher T_c s for larger VCCs, it is reasonable to look systematically for higher values of the VCC in order to obtain a higher T_c value.

More generally, we are looking for a place for chemical intuition in thinking about HTSC,³ so as to provide a reasonable direction to the experimental search for new materials.

³ For the work of four groups with a chemical and physical orientation see Refs. [10–13].

The general plan of our five-part study, entitled “Chemistry of Vibronic Coupling” is as follows: in this paper (part 1) we show, using a simple model of two harmonic potential wells, how to maximize the VCC λ^4 in the “space” of force constants, normal coordinates and reduced oscillator masses. In forthcoming papers we will then look closer at diagonal and off-diagonal VCCs h in a space of “chemical parameters” such as the electronegativity and covalent/ionic radii of the elements involved. In part 2 of the series [14] we perform quantum mechanical (QM) calculations of the dynamic *diagonal* VCC for closed shell diatomics MeX (Me = alkali metal or H, X = halogen or H). In part 3 [15] we perform QM computations of the dynamic *off-diagonal* VCC for mixed-valence and intermediate valence Me_2X systems (Me = alkali metal or H, X = halogen or H). Finally, in part 4 [16] we will focus on both diagonal and off-diagonal VCCs, looking for rules which might help to understand the influence of Me and X position in the periodic table on the value of VCC. In part 5 of the series [17], we will try to understand VCCs as molecular systems are expanded into solids.

We will be looking to build a bridge between the VCCs and electron–phonon coupling constants. In our simple considerations of the VCC in the context of superconductivity we thus hope to come all the way from simple molecular systems to solids.

2. Methods of calculations

2.1. Types of vibronic coupling constants

There are many types of VCCs (vibronic coupling constants) used. It is therefore necessary to define accurately our notation and point of interest.⁵

⁴ For definitions of λ/eV and $\lambda/eV/\text{\AA}$ see Section 2 of this paper.

⁵ For vibronic coupling in molecules and in solids see Refs. [18–20]; on the role of vibronic coupling for electronic and vibrational dynamics see Refs. [21,22]; for charge transfer processes in condensed media see Refs. [23,24]; on Jahn–Teller effect in molecules and in solid state see Refs. [25–28].

Most often a VCC is expressed in force units, and denoted as h . There may be diagonal and off-diagonal VCCs, and linear and nonlinear ones. Among them we will look closer at the *dynamic off-diagonal linear VCC* (h_{eg}^i) defined as

$$h_{eg}^i(Q_i) = \langle g | \delta H / \delta Q_i | e \rangle \quad (\text{typical units } \text{meV}/\text{\AA}) \quad (1)$$

where g and e are the diabatic electronic wave functions of two vibronically coupled electronic states, and $\delta H / \delta Q_i$ is the derivative of Hamiltonian along the normal coordinate Q_i through which coupling occurs. Usually g is assumed to be the ground state of a system. h_{eg}^i depends on geometry of a molecule; in this paper we will be interested only in a dependence of h_{eg}^i on one normal coordinate, Q_i .

If $g \equiv e$, then h_{eg}^i becomes a diagonal linear CC (h_{ee}^i):

$$h_{ee}^i = \langle e | \delta H / \delta Q_i | e \rangle \quad (\text{meV}/\text{\AA}). \quad (2)$$

The h_{ee}^i may be thought as a negative force F_e^i acting on the potential energy surface (PES) of the excited state e along normal coordinate Q_i :

$$h_{ee}^i = -F_e^i. \quad (3)$$

If one determines h_{ee}^i at the equilibrium geometry of the ground state (g_0), then h_{ee}^i becomes a derivative of the $g \rightarrow e$ excitation energy along Q_i , evaluated at g_0 :

$$h_{ee}^i = \delta E_{\text{exc}} / \delta Q_i \quad \text{at } g_0. \quad (4)$$

This definition of h_{ee}^i is close to chemical intuition; Eq. (4) says that h_{ee}^i is large when the energy of $g \rightarrow e$ excitation changes substantially between opposite phases of normal vibration i (extension and contraction of the bond from its ground state equilibrium value). Fig. 2a illustrates definition of h_{ee}^i given in Eq. (4).

Eq. (4) helps us to understand the cases when $h_{ee}^i = 0$. A given vibration i has no effect on the electronic excitation energy when the PES minimum of the excited state e is not displaced along coordinate Q_i in comparison with the PES minimum of the ground state g (Fig. 2b). One way this might be realized is when vibration i involves

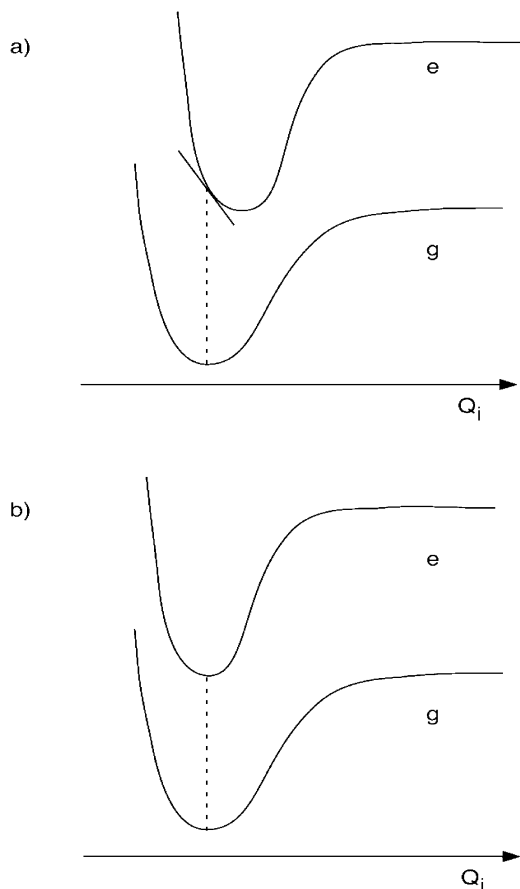


Fig. 2. Schematic PESs for the ground (g) and excited (e) states along normal coordinate Q_i : (a) case of $h_{ee}^i \neq 0$; (b) case of $h_{ee}^i = 0$.

motion of atoms whose atomic orbitals do not contribute to the molecular orbitals involved in the $g \rightarrow e$ transition. An illustration might be an organic molecule consisting of a chromophoric part and a long side aliphatic chain. The vibrations of the aliphatic chain, separated as they are from the chromophore part of a molecule, obviously have no impact on the $g \rightarrow e$ excitation energy.

When is h_{ee}^i large? Consider the $g \rightarrow e$ transition arising from a HOMO/LUMO transition. h_{ee}^i will be large for vibrations involving a given C_a-C_b bond stretch when HOMO and LUMO differ by a node across the C_a-C_b bond. It is very likely that a large C_a-C_b bond length difference between the g and e states (and consequently a strong dependence

of the $g \rightarrow e$ excitation energy on the C_a-C_b bond length) would be a consequence of such a nodal change (node in HOMO across the C_a-C_b bond, no node in LUMO or vice versa). In other words, if during an electronic transition the bond order for a given bond changes much, then only those vibrations i which involve stretching of this bond will have large h_{ee}^i .

Let us now return for a moment to off-diagonal CC h_{ge}^i . Looking at its definition (Eq. (1)) one can easily predict when h_{ge}^i vanishes. $h_{ge}^i = 0$ when:

(i) the molecular vibration i does not have the proper symmetry to couple states g and e or

(ii) the $g \rightarrow e$ transition is spin-forbidden. Of course, there is an additional simple intuitive rule for h_{ge}^i , similar to that given for h_{ee}^i :

(iii) among normal vibrational modes which may couple states g and e , the largest values of h_{ge}^i should be found for modes i involving movement of atoms whose atomic orbitals contribute substantially to MOs engaged in the $g \rightarrow e$ transition. For example, let the $g \rightarrow e$ transition be a $\pi-\pi^*$ transition in a large organic molecule. Let us concentrate at a certain C_a-C_b bond, such that contributions of p_z (π) orbitals of C_a and C_b carbon atoms to both g and e states are large. Let the contribution of p_z orbital of C_a be of the same sign in g and e , and let the contribution of p_z orbital of C_b be of the opposite sign in g and e . Under such conditions a large coupling constant h_{ge}^i should be expected for those normal modes with a significant contribution from a C_a-C_b stretch.

As we will show in the following papers, interesting correlations may be found for h_{ge}^i and h_{ee}^i for a broad range of simple molecules.

The CC which is most important in considerations of superconductivity (usually denoted λ) is expressed in energy units and defined as

$$\lambda_{eg}^i = (\lambda_{eg}^i)_v = h_{eg}^i \langle u_g | Q_i | v_e \rangle \quad (\text{meV}) \quad (5)$$

where u_g and v_e are vibrational wave functions for normal mode i , in g and e states respectively. The $\langle u_g | Q_i | v_e \rangle$ integral is computed taking u_g with vibrational quantum number equal to zero and full set of v_e (vibrational quantum number varies from 0 to ∞). Again, most often g is here the ground and e is a certain excited electronic state.

λ_{eg}^i and λ_{ee}^i (which is defined in a manner similar to λ_{eg}^i) have energy units. These parameters are central to classical superconductivity explanations, because of the BCS theory [5] relationship:

$$kT_c = 1.14 h\nu_{\text{Deb}} \exp[(\lambda \tilde{N}_F)^{-1}] \quad (6)$$

where k is the Boltzmann constant, T_c the critical superconducting temperature, ν_{Deb} the cutoff frequency of the phonon spectrum, λ the electron–phonon coupling constant ⁶ in solid decreased by coulombic repulsion of electrons, and \tilde{N}_F the density of states at the Fermi level. The product $\lambda \tilde{N}_F$ is often called the pairing potential, since it controls the condensation of electrons into boson pairs. In other words, phonons open energy gaps at the Fermi level (the magnitude of the gaps may vary for different vibrations of the lattice). For us it is essential to note that a large electron–phonon coupling constant λ leads to a high superconducting transition temperature T_c . The present paper is devoted to λ_{eg}^i , a counterpart of BCS λ in molecular systems.

The remaining kind of CC which is often used is a dimensionless one (denoted most often as g_{eg}^i) and defined as

$$g_{eg}^i = [1/\hbar\omega_i] \lambda_{eg}^i \quad (7)$$

where $\hbar\omega_i$ is the energy of vibration i . Definition of g_{ee}^i is analogous to that given in Eq. (7). While we are not directly interested in the g_{eg}^i and g_{ee}^i , they are widely used in resonance Raman studies [29], theory of CT complexes [30] and in the Marcus theory of electron transfer [31] when analyzing contributions from various vibrations to distortion of a molecule upon electron transfer (most often g_{ee}^i is point of interest in studies based on so-called crude Born–Oppenheimer approximation).

So far we have introduced here the coupling constants for a single normal mode i ($h_{ee}^i, h_{eg}^i, \lambda_{eg}^i, \lambda_{ee}^i, g_{eg}^i, g_{ee}^i$). These are *linear* CCs. There are cases, when CCs of higher order than linear should be considered. The simplest *quadratic* off-diagonal CC is defined as

⁶ Both diagonal and off-diagonal vibronic coupling constants enter BCS considerations as mentioned above.

$$h_{eg}^{ij} = \langle g | \delta^2 H / \delta Q_i \delta Q_j | e \rangle \text{ (meV/\AA}^2 \text{)}, \quad (8)$$

with its diagonal counterpart

$$h_{ee}^{ij} = \langle e | \delta^2 H / \delta Q_i \delta Q_j | e \rangle \text{ (meV/\AA}^2 \text{)}. \quad (9)$$

Now, i and j are two normal vibrational modes. In case $i \neq j$, h_{ee}^{ij} describes vibronic coupling of e and g states through an i and j combination mode. When $i = j$, h_{ee}^i describes vibronic coupling of e and g through i 's first overtone. Of course, quadratic λ_{eg}^{ij} and λ_{ee}^{ij} may be easily derived from both h_{eg}^{ij} and h_{ee}^{ij} , respectively. In the present and forthcoming papers [14–16] in our series ‘‘Chemistry of vibronic coupling’’ we will not consider quadratic and higher CCs.

As noted earlier, our main interest will be in h_{ee}^i , h_{eg}^i and λ_{eg}^i (especially when a $g \rightarrow e$ transition has charge-transfer character). The central focus of this paper is λ_{eg}^i .⁷

The literature in this field is diverse, traversing chemistry and physics. There are many current nomenclatures in place for h , g and λ . We have taken time here, with apologies to the experts in the field, to delineate clearly the relationships between the different measures of vibronic coupling.

Let us present now the simple model used for λ_{eg}^i calculations.

2.2. Model for calculations of the λ_{eg}^i

Imagine two electronic states g and e described by harmonic potential curves along coordinate Q_i (Fig. 3a). We introduce the variables k , ΔQ , c , and m . k has physical meaning of a force constant for vibration i in both e and g states, ΔQ is the displacement between the minima of e and g states along Q_i , c is the vertical (energy) displacement between the minima of e and g states, and m is a

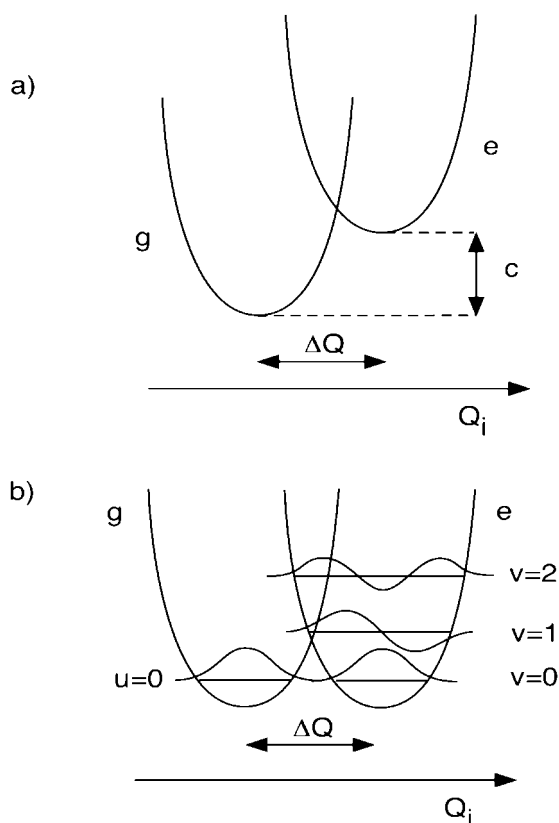


Fig. 3. Schematic PESs for electronic states g and e for the model used in this paper; (a) $c \neq 0$, (b) $c = 0$. See text for further details.

reduced mass for vibration i . In our diabatic model we assume, similarly to Marcus [33], that the force constants in states g and e are the same.⁸ When $c = 0$ we have the case of a degenerate double-minima potential well, realized for asymmetric mixed-valence compounds (see Fig. 3b). We want to find λ_{eg}^i according to Eq. (5), varying k , ΔQ , c , and m as widely as possible. One immediately notices that parameter c does not change the value of λ_{eg}^i (neither the h_{eg}^i nor the $\langle u_g | Q_i | v_e \rangle$ term) in our model (although it contributes to the $g \rightarrow e$

⁷ We consider here a special case when the same vibration is Herzberg–Teller active and involved in a geometry change upon electronic excitation. In this context note an opposite case, when a Herzberg–Teller active mode does not form progression in the electronic spectrum, and the progression-forming frequencies do not effect vibronic perturbations. See an interesting contribution on the phenanthrene 3400 Å system in Ref. [32].

⁸ This approximation is usually fulfilled with 10% accuracy, but deviations as big as $\pm 30\%$ are known. We will discuss later the qualitative impact of these deviations on the value of λ , while now we will remain within the above assumption.

excitation energy). Thus, we will exclude parameter c from the space of variables, reducing it to k , ΔQ and m . Phenomenologically, these three parameters fully describe λ_{eg}^i in any molecular system within a diabatic harmonic potential model.

We have performed a scan of values of the VCC λ_{eg}^i in the space of the above molecular parameters. For this purpose a short program in the Python programming language has been written. Our algorithm computes independently the h_{eg}^i term and $\langle u_g | Q_i | v_e \rangle$ term. The h_{eg}^i term is simply [34]

$$h_{eg}^i = k\Delta Q, \quad (10)$$

which requires no integration and is obviously m -independent.

The $\langle u_g | Q_i | v_e \rangle$ term is found by a numerical integration procedure.⁹ The algorithm used was Romberg's extension to the trapezoidal rule for better computational efficiency. A vibrational wave function for a quantum oscillator is

$$\Psi_v(Q_i) = N_v H_v(y) \exp(-y^2/2) \quad (11)$$

where

$$N_v = \{(2^v v!)^{-1} \Pi^{1/2}\}^{1/2} \quad (12)$$

is the normalization factor.

$$H_v(y) = (-1)^v \exp(y^2) d^v [\exp(-y^2)] / dy^v \quad (13)$$

is Hermite's polynomial and

$$y = [m\omega_i 2\Pi/\hbar]^{1/2} Q, \quad (14)$$

$$\omega = (k/m)^{1/2} \quad (15)$$

where $\omega_i/2\Pi$ is the frequency of vibration i , and v is the vibrational quantum number.

Our algorithm computes the $\langle u_g | Q_i | v_e \rangle$ term taking up to 15th order Hermite polynomials. We have observed that due to the normalization factor N_v (strongly decreasing with v) the contribution from higher orders than the 15th is negligible. The integration limits were usually $(-7, +7)$ bohrs with a 0.01 bohr grid, providing fast convergence. For large values of k and small values of ΔQ , huge integration limits were not necessary. Hence,

Table 1

Values of h and λ as a function of k and ΔQ for three different masses: $m = 1, 10, 100$ amu

k (hartree/ bohr ²)	ΔQ (bohr)	h (hartree/ bohr)	λ (hartree)
<i>m</i> = 1			
5	0.27	1.35	0.26
20	0.19	3.8	0.52
50	0.15	7.5	0.82
100	0.13	13	1.16
300	0.1	30	2
500	0.09	45	2.59
700	0.08	56	3.06
1000	0.07	70	3.66
<i>m</i> = 10			
5	0.15	0.75	0.08
50	0.08	4	0.26
300	0.055	16.5	0.63
500	0.05	25	0.82
700	0.045	31.5	0.96
1000	0.04	40	1.16
<i>m</i> = 100			
5	0.09	0.45	0.025
50	0.05	2.5	0.08
300	0.03	9	0.2
500	0.025	12.5	0.26
1000	0.02	20	0.36

smaller integration limits of ± 3 to 5 bohrs were used. Finally, the $\langle u_g | Q_i | v_e \rangle$ term was multiplied by h_{eg}^i to get λ_{eg}^i .

Our calculations were performed in atomic units of h , atomic mass units, hartrees and bohrs. In these units: $k = 1$ hartree/bohr² = 1556.7 N/m = 15.567 mDyne/Å. Numerical results are shown in Table 1.

3. Results and discussion

Fig. 4 presents a plot of λ_{eg}^i and its components: $\langle u_g | Q_i | v_e \rangle$ and h_{eg}^i as a function of ΔQ for $k = 5$ and $m = 1$. This plot is central to our considerations. Its main features can be easily deduced without calculations. Indeed, this is how we really came a long way toward understanding of λ_{eg}^i , before any computations were performed.

It may be seen in Fig. 4 that there appears a *maximum* in λ_{eg}^i , at about 0.25 bohr. This maxi-

⁹ Analytical formulas have been obtained in Ref. [35].

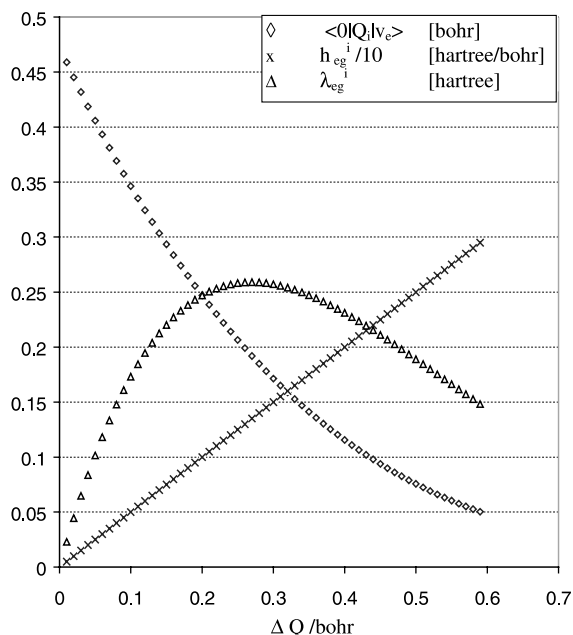


Fig. 4. Plots of and its components: $\langle u_g | Q_i | v_e \rangle$ and h_{eg}^i as a function of ΔQ for $k = 5$ and $m = 1$; h_{eg}^i has been divided by a factor of 10 to present these three plots on the same scale, although each of them has obviously different units.

imum originates from the *opposing* behavior of h_{eg}^i (which, since $h_{eg}^i = k\Delta Q$, grows with increasing ΔQ) and $\langle u_g | Q_i | v_e \rangle$ (which decreases with increasing ΔQ). The product of these two terms has a maximum along ΔQ . Very similar plots (not shown here) may be obtained for λ_{eg}^i and its components: $\langle u_g | Q_i | v_e \rangle$ and h_{eg}^i as a function of k for ΔQ , $m = \text{constant}$. Again, for small values of k ($k \approx 0$), the overall λ_{eg}^i is close to 0, due to the small h_{eg}^i term. For large values of k , the $\langle u_g | Q_i | v_e \rangle$ term is now very small, giving rise to a small λ_{eg}^i . Again, there is some optimal value of k , yielding maximum λ_{eg}^i . The existence of a maximum in λ_{eg}^i in Fig. 4 is very interesting in the context of superconductivity. It means that one needs to find an optimal value of ΔQ (hereafter called ΔQ_{opt}) for a given k and m , or an optimal value of k (hereafter called k_{opt}) for a given ΔQ and m , in order to attain a maximum value of the coupling constant λ_{eg}^i .

Let us now plot the $(\Delta Q, k)$ points providing maximum λ_{eg}^i for three different values of m ($m = 1$ amu, 10 amu, 100 amu). As it may be seen in Fig. 5,

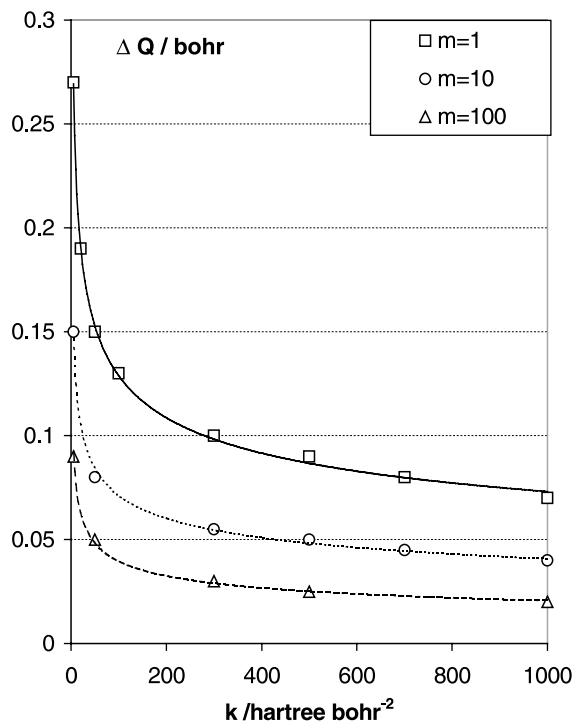


Fig. 5. $(\Delta Q, k)$ points providing maximum λ_{eg}^i s. Three different values of reduced oscillator mass, m , ($m = 1, 10, 100$ amu) have been assumed.

the position of ΔQ_{opt} is a *monotonic and decreasing function* of k for all three reduced masses. The necessity of ΔQ tuning for given value of k s in order to maximize λ_{eg}^i may be easily understood. For very steep parabolas describing the PES of electronic states g and e , one needs to provide small ΔQ_{opt} to have $\langle u_g | Q_i | v_e \rangle$ large enough.

On the other hand, it is necessary to separate the minima of shallow parabolas to obtain large h_{eg}^i (and hence attain large λ_{eg}^i). Interestingly, the position of “optimal” ΔQ_{opt} for a given k varies with m . At a given k , the larger m , the smaller ΔQ_{opt} . Or, alternatively, at given ΔQ , the larger m , the smaller k_{opt} . The hyperbolic-like behavior of optimal (i.e. those providing highest λ_{eg}^i s) $(\Delta Q, k)$ points may be understood considering four simple relationships:

$$\lambda_{eg}^i = 0 \quad \text{for } k = 0 \quad (\text{ordinate axis in Fig. 5}), \quad (16a)$$

$$\lambda_{eg}^i = 0 \quad \text{for } \Delta Q = 0 \quad (\text{abscissa axis in Fig. 5}), \quad (16b)$$

$$\lambda_{eg}^i = 0 \quad \text{for } k \rightarrow \infty \quad \text{and} \quad \Delta Q \rightarrow \infty, \quad (16c)$$

$$\lambda_{eg}^i \text{ should be a continuous function of } k \text{ and } \Delta Q. \quad (16d)$$

Computational data suggest that with simultaneous k and ΔQ increase, the $\langle u_g | Q_i | v_e \rangle$ term goes to zero faster than the h_{eg}^i term goes to infinity (Eq. (16c)).

Fig. 5 does not tell us about λ_{eg}^i values at “optimal” $(k, \Delta Q)$ points. Consider such λ_{eg}^i , plotted as a function of $\sqrt{k/m}$ (Fig. 6).

As may be seen in Fig. 6, λ_{eg}^i is a linear function of $\sqrt{k/m}$ for “optimal” $(k, \Delta Q)$ points (of course, it is not a linear function of $\sqrt{k/m}$ for any $(k, \Delta Q)$ points). The largest λ_{eg}^i of 3.7 hartree (within the space of k , m and ΔQ monitored by us) is reached for $k = 1000$ hartree/bohr² $\approx 15.6 \times 10^3$ mDyne/Å, for $m = 1$ amu and at ΔQ_{opt} (about 0.04 bohr). Of course, 1000 hartree/bohr² is a force constant

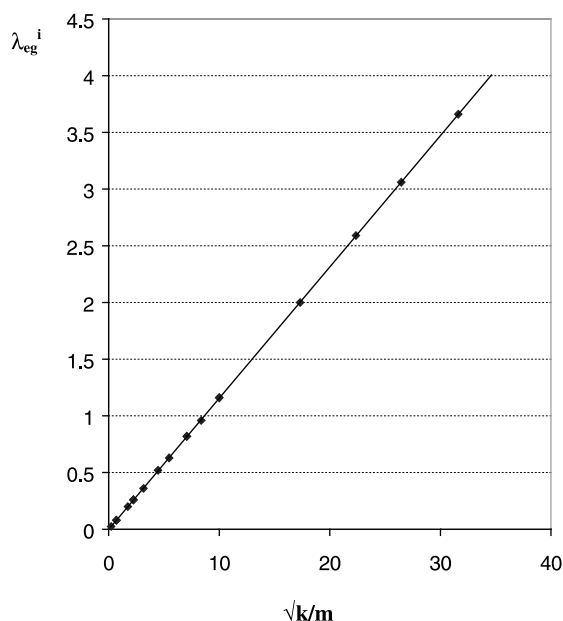


Fig. 6. Plot of λ_{eg}^i values at “optimal” $(k, \Delta Q)$ points as a function of $\sqrt{k/m}$.

value which cannot be reached by any molecular or extended system. It is two orders of magnitude larger than the force constant for the nitrogen molecule N_2 (≈ 3 hartree/bohr²). That extreme upper k limit was not realistic, but chosen only to illustrate clearly the trend for λ_{eg}^i which holds regardless of the $(k, \Delta Q)$ – space probing. Let us proceed, limiting ourselves to a reasonable space of ks in the range from 0 to 5 hartree/bohr². For a typical chemical system with $k = 1$ hartree/bohr² and $m = 10$ amu, λ_{eg}^i will decrease to 0.037 hartree (about 1 eV) for “optimal” ΔQ . For “nonoptimal” ΔQ , values of λ_{eg}^i will be smaller than this.

There is one more question that begs to be answered: can h_{eg}^i be a monotonic indicator of large λ_{eg}^i s? Let us put the problem in other way: if k increases and ΔQ simultaneously decreases (k and ΔQ are optimal for each other), what happens to the h_{eg}^i values? The answer to this question is given in Fig. 7.

As may be seen in Fig. 7, if optimal $(k, \Delta Q)$ are provided, the increase in h_{eg}^i s is connected with

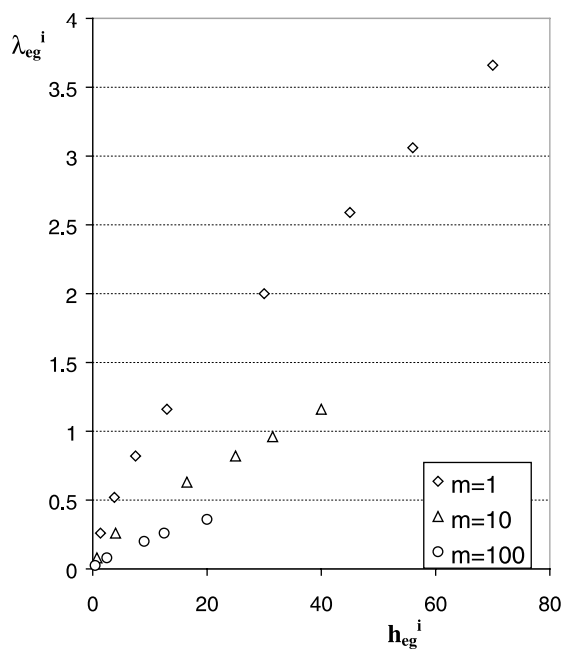


Fig. 7. Illustration of the λ_{eg}^i vs h_{eg}^i monotonic relationship for three masses ($m = 1, 10, 100$ amu) at $(k, \Delta Q)$ points optimal for given h_{eg}^i .

simultaneous monotonic (although less than linear) increase of λ_{eg}^i . Let us summarize the results obtained. The perspectives for maximizing the coupling constant λ_{eg}^i are as follows:

(i) there exists a maximal value of λ_{eg}^i which may be found for a given force constant k by providing the appropriate ΔQ_{opt} ; ΔQ_{opt} decreases with k increasing.

(ii) λ_{eg}^i may be maximized by increasing the k/m ratio with simultaneous adjustment of ΔQ .

(iii) λ_{eg}^i may be maximized for given m by increasing h_{eg}^i , but k should be precisely adjusted to ΔQ .

These rules may be translated into chemical language as follows:

(iv) large values of λ_{eg}^i in mixed-valence molecular systems should be sought for in systems with strong multiple bonds (large ks) built of light elements (small ms). The ΔQ should be precisely adjusted for a given (k, m) pair. The larger the expected values of λ_{eg}^i , the greater precision in ΔQ tuning is necessary.

One can see two serious problems in applying the qualitative understanding reached, even for molecules. These are connected with the necessity of precise ΔQ adjustment for large k . Under- or overestimation of ΔQ results in a strong decrease of λ_{eg}^i . The problems are as follows:

(1) Many molecules with large k ¹⁰ prefer to be symmetric. Exceptions from a “self-symmetrization” of the system for large k are only found among molecules with large h_{eg}^i such as symmetric linear F_3 or F_2H radicals [16]. Such molecules are, however, extremely unstable toward decomposition [16].

(2) Another complication is hidden in the real adiabatic (and not diabatic, as previously assumed) character of the g and e states, which mix, creating two nondegenerate states: the real ground and excited state of a system (see next section). According to the simplest theory using adiabatic potentials [36], strong adiabaticity influences ΔQ

in a major way, usually leading to *symmetrization* of a molecule along Q_i . Given adiabaticity as one more independent parameter, it is not easy to guess and provide the “optimum” value of ΔQ for given molecule.

These examples show how difficult it will actually be to design large λ_{eg}^i by playing with ΔQ .

Our observations of the existence of *optimal* ΔQ for given k have an interesting counterpart in studies of high-temperature superconductors. As experimental T_c vs doping (x) and T_c vs external pressure (p) curves show, there exists an *optimal* level of doping and an optimal external pressure applied which allow T_c *maximization* [37,38]. Either too small or too large values of x and p strongly influence bond distances and lead to disappearance of the HTSC phenomenon. On the other hand, experimental data (mainly for the well-studied cuprates [39,40]) indicate a strong correlation of HTSC with lattice instability and phase transitions in these complex solid state systems.

Let us now briefly discuss the qualitative impact of deviations from diabaticity and harmonicity on final value of λ_{eg}^i .

3.1. The effects of deviations from diabaticity and harmonicity on λ_{eg}^i

In the simple model used, we have assumed harmonicity of the vibrations in g and e states along Q_i (with force constants equal in both states, $k_e = k_g$) and diabaticity (PESs for states g and e cross at $Q_i = 0$, see Fig. 3b). We would like to discuss now briefly and in a qualitative way the impact of breakdown of these assumptions on the value of λ_{eg}^i .

(i) What if $k_e \neq k_g$? Since we decided to look for large λ_{eg}^i s among systems with strong multiple bonds (providing large ks), we should not be bothered by eventual breakdown of the $k_e = k_g$ assumption. To demonstrate this, consider a typical mixed-valence (MV) system of type $\{M^{n+} - A^{m-} - M^{(n+)+}\}$. Given the same σ skeleton in two “units” differing by one electron ($M^{n+} - A^{m-}$ and $A^{m-} - M^{(n+)+}$), the differences in stretching force constants for the above units originate exclusively from the partial π bonding. Since π bonds are

¹⁰ We mean here k , which has been used by us to describe curvature of parabolas in a diabatic potential model, and not a real force constant for antisymmetric stretch of F_3 or F_2H . Obviously the latter is imaginary for both systems.

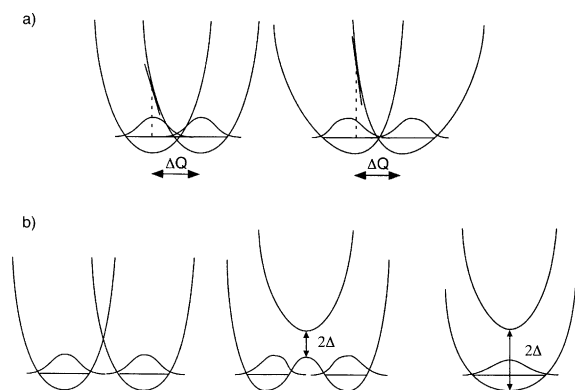


Fig. 8. Impact of (a) anharmonicity and (b) increasing adiabaticity, on PES and vibrational wave functions in a system with degenerate double-minima potential wells.

much weaker than σ bonds, stretching force constants for the above units will not differ much. Hence, our assumption of $k_e = k_g$ will be violated only slightly.

(ii) What if vibrations are not harmonic? The effect of anharmonicity of vibrations on our model is shown in Fig. 8a.

It seems that anharmonicity has a double impact on λ_{eg}^i : through h_{eg}^i and also through $\langle u_g | Q_i | v_e \rangle$. While anharmonicity increases h_{eg}^i (by comparison with harmonic case), it diminishes the $\langle u_g | Q_i | v_e \rangle$ term. The result of the interplay of h_{eg}^i and $\langle u_g | Q_i | v_e \rangle$ (though the influence of these two seems to cancel to some extent) is difficult to deduce. And, in experiment, is difficult to control. More exact studies (using Morse potentials for example) might be performed in order to determine quantitatively the role of anharmonicity for λ_{eg}^i .

(iii) What if the system is adiabatic? The effect of increasing adiabaticity is illustrated in Fig. 8b [41]. Among factors discussed so far, adiabaticity (measured by electronic coupling parameter Δ [34,36]) undoubtedly has the strongest impact on λ_{eg}^i . Again, its role is not easily quantified. Adiabaticity influences values of h_{eg}^i , ΔQ and $\langle u_g | Q_i | v_e \rangle$, i.e. λ_{eg}^i and Δ are not independent parameters. In our opinion, the most significant influence of increasing adiabaticity on λ_{eg}^i is connected with the tendency for symmetrizing a molecule even for large h_{eg}^i (a mixed-valence system becomes an intermediate-valence system). This means that large

λ_{eg}^i may be also hidden in symmetric systems, contrary to our predictions based on a simplistic diabatic potential model.

4. Conclusions

Using a simple diabatic model of two equivalent electronic states with harmonic PESs, we analyze values of the dynamic off-diagonal VCC (λ_{eg}^i) as a function of three parameters: force constant (k), reduced oscillator mass (m) and displacement between two minima along the normal coordinate of a coupling mode Q_i (ΔQ). We show that for each k there is only one ΔQ which maximizes λ_{eg}^i . Existence of a maximum in the λ_{eg}^i originates from the opposing behavior of h_{eg}^i and $\langle g | \delta H / \delta Q_i | e \rangle$ factors in $(k, \Delta Q)$ space.

In searching for large λ_{eg}^i s we are then led to adjusting properly small ΔQ s in systems with strong multiple bonds (large ks). It also emerges that λ_{eg}^i correlates linearly with $\sqrt{(k/m)}$. Hence, one should build system of light elements so to maximize λ_{eg}^i . However, these conditions are very hard to realize experimentally, because real systems with large ks either have a tendency (a) toward symmetrization along Q_i , or (b) to chemical decomposition. ΔQ and k are not independent parameters, as well.

The results presented here may be useful in the experimental search for HTSC, in delimiting the space of element combinations which should be investigated. Of course, superconductivity is a very complex solid state physical phenomenon. It cannot be explained exclusively by a simple diabatic, harmonic potential model such as that we used in our simulations. This is why in parts 2, 3 and 4 of this series we will computationally examine dynamic linear VCCs in real QM molecular systems.

Acknowledgements

This research was conducted using the resources of the Cornell Theory Center, which receives funding from Cornell University, New York State, the National Center for Research Resources at the National Institutes of Health, the National Science

Foundation, the Defense Department Modernization Program, the United States Department of Agriculture, and corporate partners. This work was supported by the Cornell Center for Materials Research (CCMR), a Materials Research Science and Engineering Center of the National Science Foundation (DMR-9632275). W. Grochala thanks also to Kosciuszko Foundation for financial support. Andrea Ienco is acknowledged for writing a preliminary version of an integration program.

References

- [1] G. Herzberg, E. Teller, *Z. Phys. Chem. B* 21 (1933) 410.
- [2] G. Herzberg, H.C. Longuet-Higgins, *Discuss. Faraday Soc.* 35 (1963) 77.
- [3] H.C. Longuet-Higgins, *Proc. R. Soc. London Ser. A* 344 (1975) 147.
- [4] W. Siebrand, M. Zgierski, in: E.C. Lim (Ed.), *Excited States*, vol. 4, Academic Press, New York, 1979.
- [5] J. Bardeen, L.N. Cooper, J.R. Schrieffer, *Phys. Rev.* 108 (1957) 175.
- [6] J.G. Bednorz, K.A. Müller, *Z. Phys. B* 64 (1986) 189.
- [7] V. Mereghelli, S.Y. Savrasov, *Phys. Rev. B* 57 (1998) 14453.
- [8] N. Garro, A. Cantarero, M. Cardona, T. Ruf, A. Göbel, C. Lin, K. Reimann, S. Rübenacke, M. Steube, *Solid State Commun.* 98 (1996) 27.
- [9] B. Chakraverty, T. Ramakrishnan, *Physica C* 282–287 (1997) 290.
- [10] K.A. Müller, in: E. Sigmund, K.A. Müller (Eds.), *Phase Separation in Cuprate Superconductors*, Proc., Springer, Berlin, 1993, p. 1.
- [11] A. Simon, *Angew. Chem. Int. Ed. Engl.* 36 (1997) 1788.
- [12] A.W. Sleight, *Acc. Chem. Res.* 28 (1995) 103.
- [13] J.K. Burdett, *Inorg. Chem.* 32 (1993) 3915.
- [14] W. Grochala, R. Hoffmann, *New J. Chem.* 25 (2001) 108.
- [15] W. Grochala, R. Hoffmann, *J. Phys. Chem. A* 104 (2001) 9740.
- [16] W. Grochala, R. Hoffmann, *Phys. Chem. Chem. Phys.*, submitted for publication.
- [17] W. Grochala, R. Hoffmann, P.P. Edwards, in preparation.
- [18] G. Herzberg, *Molecular Spectra and Molecular Structure*, vol. 3, *Electronic Spectra and Electronic Structure of Polyatomic Molecules*, van Nostrand Reinhold Company, New York, 1966.
- [19] G. Fischer, *Vibronic Coupling*, Academic Press, London, 1984.
- [20] H. Köppel, L.S. Cederbaum, W. Domcke, *J. Chem. Phys.* 89 (1988) 2023.
- [21] W. Domcke, G. Stock, Theory of ultrafast nonadiabatic excited-state processes and their spectroscopic detection in real time, in: I. Prigogine, S.A. Rice (Eds.), *Advances in Chemical Physics*, vol. 100, Wiley, New York, 1997.
- [22] R. Schneider, W. Domcke, H. Köppel, *J. Chem. Phys.* 92 (1990) 1045.
- [23] J. Ulstrup, Charge transfer processes in condensed media, in: G. Berthier, M.J.S. Dewar, H. Fisher, K. Fukui, H. Hartmann, H.H. Jaffe, J. Jortner, W. Kutzelnigg, K. Ruedenberg, E. Scrocco, W. Zeil (Eds.), *Lecture Notes in Chemistry*, vol. 10, Springer, Berlin, 1979.
- [24] H.E.M. Christensen, L.S. Conrad, J.M. Hammerstad-Pedersen, J. Ulstrup, Charge transfer in chemistry and biology; a selective overview, in: M.P. Tosi, A.A. Kornyshev (Eds.), *Condensed Matter Physics Aspects of Electrochemistry*, World Scientific, Singapore, 1991.
- [25] H.A. Jahn, E. Teller, *Proc. R. Soc. London Ser. A* 161 (1937) 220.
- [26] L.R. Falvello, *J. Chem. Soc. Dalton Trans.* (1997) 4463.
- [27] I.B. Bersuker, *The Jahn–Teller Effect and Vibronic Interactions in Modern Chemistry*, Plenum Press, New York, 1984.
- [28] R. Englman, *The Jahn–Teller Effect*, Wiley, New York, 1972.
- [29] P.J. Reid, C. Silva, P.F. Barbara, L. Karki, J.T. Hupp, *J. Phys. Chem.* 99 (1995) 2609.
- [30] K. Kulinowski, I.R. Gould, A.B. Myers, *J. Phys. Chem.* 99 (1995) 9017.
- [31] A. Klimkans, S. Larsson, *Chem. Phys.* 189 (1994) 25.
- [32] D.P. Craig, G.J. Small, *J. Chem. Phys.* 50 (1969) 3827.
- [33] R.A. Marcus, *J. Chem. Phys.* 24 (1956) 966.
- [34] K.Y. Wong, P.N. Schatz, A dynamic model for mixed-valence compounds, in: S.J. Lippard (Ed.), *Progress in Inorganic Chemistry*, vol. 28, Wiley, New York, 1981, p. 369.
- [35] M.K. Grover, R. Silbey, *J. Chem. Phys.* 52 (1970) 2099.
- [36] I.B. Bersuker, V.Z. Polinger, in: V.I. Goldanskii (Ed.), *Vibronic Interactions in Molecules and Crystals*, Springer, Berlin, 1983.
- [37] J. Gopalakrishnan, in: A.M. Herman, J.V. Jakhmi (Eds.), *Thallium-Based High-Temperature Superconductors*, Marcel Dekker, Inc., New York, 1995, p. 7.
- [38] N.E. Moulton, E. Skeleton, in: A.M. Herman, J.V. Jakhmi (Eds.), *Thallium-Based High-Temperature Superconductors*, Marcel Dekker, Inc., New York, 1995, p. 437.
- [39] E. Sigmund, K.A. Müller (Eds.), *Phase Separation in Cuprate Superconductors*, Proc., Springer, Berlin, 1993.
- [40] R.S. Markiewicz, *Physica C* 162–164 (1989) 215.
- [41] H.C. Longuet-Higgins, in: H.W. Thompson (Ed.), *Advances in Spectroscopy*, vol. 2, Interscience, New York, 1961, p. 429.